https://doi.org/10.5194/essd-2026-128
Preprint. Discussion started: 9 March 2026

Open Access Earth System Science Data Discussions

A 500-m crop water requirement and irrigation water demand dataset for 25 crop types in the Yellow River Basin (2000–2020): Revealing significant underestimation from incomplete crop coverage

Shizhen Tang[1,2,3,4], Ziying Li[1,2], Xueyan Sun[5], Lun Luo[6], Liwen Zhang[1,2,5], Yanghai Duan[7], Jiaqi Wang[1,2], Qian Li[3], Hongbo Zhang[1,2,3*]

[1] State Key Laboratory of Efficient Utilization of Agricultural Water Resources, China Agricultural University, Beijing, China
[2] College of Water Resources & Civil Engineering, China Agricultural University, Beijing, China
[3] Xinjiang Key Laboratory of Water Cycle and Utilization in Arid Zone, Xinjiang Institute of Ecology and Geography, Chinese Academy of Sciences 830011, Urumqi, China
[4] Water Affairs Bureau of Baiyun District, Guangzhou, China
[5] Yantai Research Institute, China Agricultural University, Yantai, China
[6] Bomi Field Scientific Observation and Research Station for Alpine Mountain Geo-Hazard Chains, Institute of Mountain Hazards and Environment, Chinese Academy of Sciences, Chengdu, China
[7] Middle Yarlung Zangbo River Natural Resources Observation and Research Station of Tibet Autonomous Region, Research Center of Applied Geology of China Geological Survey, Cheng Du 610036, China

Correspondence to: Hongbo Zhang (zhanghongbo@cau.edu.cn)

https://doi.org/10.5194/essd-2026-128
Preprint. Discussion started: 9 March 2026

Open Access Earth System Science Data Discussions

Abstract. Accurate estimation of irrigation water demand (IWD) is fundamental for sustainable water resources management in water-scarce agricultural regions. However, existing IWD assessments typically consider only a limited number of major crops, potentially leading to systematic underestimation of basin-scale water demand. This study develops a comprehensive high-resolution (500 m) dataset of crop water requirement (CWR, equivalent to the net irrigation water requirement, i.e., crop evapotranspiration minus effective precipitation) and IWD (CWR divided by irrigation water use efficiency) for the Yellow River Basin (YRB) covering 25 crop types from 2000 to 2020. We first evaluated eight remote sensing-based cropland datasets against statistical records from 135 administrative units, identifying the Global Land Analysis and Discovery (GLAD) dataset as optimal. CWR and IWD were estimated using the FAO Penman-Monteith approach with spatially explicit crop coefficients and spatiotemporally dynamic irrigation water use efficiency coefficients. The dataset provides two complementary versions: a sown area-based version reflecting the full theoretical agricultural water gap (multi-year average CWR and IWD of 548.3×10^8 m^3 and 1086.8×10^8 m^3, respectively), and an irrigated area-based version constrained by actual irrigation extent (258.6×10^8 m^3 and 508.4×10^8 m^3), broadly consistent with independent estimates of actual irrigation water consumption. Our results reveal that considering only five major crops would underestimate CWR and IWD by approximately 33% and 34%, respectively, with the largest underestimation in the upper reach (approximately 45%). More importantly, incomplete crop coverage not only causes quantitative bias but also misrepresents temporal dynamics, yielding opposite trend directions in some sub-basins. Sensitivity analysis indicates that 12–15 crop types are required to capture over 90–95% of basin-scale water demand, with vegetables and tubers ranking among the top six contributors despite being frequently omitted in previous studies. The dataset (Tang and Zhang, 2026) is publicly available at https://doi.org/10.5281/zenodo.18628324.

https://doi.org/10.5194/essd-2026-128
Preprint. Discussion started: 9 March 2026

Open Access Earth System Science Data Discussions

1 Introduction

Agricultural irrigation is the largest freshwater consumer globally, accounting for approximately 70% of total freshwater withdrawals (Siebert et al., 2010). Irrigation plays an important role in ensuring food security, especially under climate change and population growth (Kadiresan and Khanal, 2018; Lutz et al., 2022). Thus, accurate estimation of crop water requirement (CWR, defined in this study as crop evapotranspiration minus effective precipitation over the growing season, equivalent to the "net irrigation water requirement" in FAO-56 terminology, representing the water deficit that must be supplied through irrigation) and irrigation water demand (IWD, i.e., CWR divided by irrigation water use efficiency coefficient) is fundamental for sustainable water resources management (De Wrachien et al., 2021; Zha et al., 2025).

Accurate estimation of IWD in large river basins is a common challenge worldwide, particularly in water-scarce regions where agriculture competes with other sectors for limited water resources (Wada et al., 2013). This challenge is particularly evident in the Yellow River Basin (YRB), which covers approximately 795,000 km^2 in northern China. The YRB is a critical grain production base contributing 35.4% of China's total grain output, yet faces severe water scarcity with per capita water resources less than 30% of the national average (Hu et al., 2012). Agricultural irrigation dominates water consumption in the basin, accounting for over 71% of total water withdrawals (Fang and Li, 2019). This conflict between food production and water availability makes spatially detailed IWD assessment increasingly urgent.

Extensive research has been conducted on IWD estimation at regional to global scales, employing various approaches including the FAO Penman-Monteith method (Allen et al., 1998; Fan et al., 2025), process-based crop models such as AquaCrop (Pirmoradian et al., 2020) and SWAT (Uniyal and Dietrich, 2019), and the agricultural ecological zone (AEZ) model (Xu et al., 2019). Among these, the FAO Penman-Monteith method is the most widely adopted approach due to its clear physical basis and relatively modest data requirements, making it particularly suitable for large-scale IWD estimation where detailed field-level observations are unavailable. These studies have provided valuable insights into the spatiotemporal dynamics of IWD and its responses to climate variability. For the YRB specifically, previous studies have examined the relationship between CWR and meteorological drought across typical irrigation districts (Wang et al., 2016), and revealed increasing trends in CWR for major crops including spring wheat, winter wheat, and maize over the past decades driven by rising temperatures and changing precipitation patterns (Liu et al., 2022). Meanwhile, the growing availability of multi-source remote sensing products has substantially improved the spatial representation of cropland distribution, enabling more spatially explicit IWD estimation (Peng et al., 2023; Xuan et al., 2023; Tu et al., 2024; Hung et al., 2025). However, despite this progress, several critical limitations persist in existing IWD assessments, particularly for the YRB (Table 1).

The most fundamental limitation lies in the incomplete coverage of crop types. As shown in Table 1, most regional IWD assessments consider only 2–8 major crops due to data availability constraints, and few have validated their underlying cropland data against independent references (Jia et al., 2022; Fan et al., 2025; Niu et al., 2022; Hou et al., 2025; Zhao et al., 2025). For instance, Shen et al. (2013) analyzed five major crops (wheat, maize, cotton, oilseed and sugar beet) in Northwest China. For the

https://doi.org/10.5194/essd-2026-128
Preprint. Discussion started: 9 March 2026

YRB, Liu et al. (2022) estimated IWD for four crops (spring wheat, winter wheat, spring maize, and summer maize), which cover approximately 66% of total cropland area. However, the remaining crops such as soybean, vegetables, potatoes, millet, and sorghum, are systematically excluded from these estimates. While individually these crops may occupy relatively small areas, collectively they may contribute substantially to basin-scale water consumption due to their diverse water requirements and growing seasons. Although some studies have incorporated more crop types (>20 categories) from global databases such as MIRCA2000 (Qin et al., 2020; Zhuo et al., 2016), they typically rely on temporally static cropland area data that cannot capture interannual variations in crop structure and associated IWD dynamics. Importantly, the magnitude of IWD underestimation resulting from this incomplete crop coverage has never been quantified. This knowledge gap may introduce systematic bias into basin-scale water allocation.

Second, significant uncertainties remain in the remote sensing-based cropland products that underpin spatially explicit IWD estimation. Since cropland distribution serves as the spatial basis for allocating crop-specific sown area from statistical records to grid cells (Zha et al., 2025), errors in cropland datasets propagate directly into IWD estimates. Yet most regional studies rely on a single cropland product without systematic accuracy validation (Zha et al., 2025; Qin et al., 2020; Fan et al., 2025; Liu et al., 2015). Recent comparative studies have revealed substantial discrepancies among existing products (Liu et al., 2025). For instance, Yang and Huang (2021) reported that cropland F1 scores varied from 58.64% to 75.64% across four widely-used datasets in China, while Tu et al. (2024) identified significant inconsistencies particularly in the Loess Plateau of the YRB. Furthermore, publicly available high-resolution IWD datasets remain scarce for major river basins, with most existing products operating at coarse spatial resolution (≥5 km) (Zhuo et al., 2016; Hou et al., 2025).

Third, the spatial heterogeneity of crop-specific parameters and irrigation water use efficiency coefficient (*IWUEC*) is often inadequately addressed in existing studies. For instance, crop coefficients (K_c) are frequently applied as single values across large areas, including the YRB (Liu et al., 2022), ignoring substantial spatial variability in crop phenology. Similarly, *IWUEC* is often treated as constant despite its inherent variability with economic development, irrigation technology, and management practices (Fan et al., 2025; Shen et al., 2013; Wada et al., 2013). Since IWD equals crop water demand divided by *IWUEC*, these simplifications can introduce considerable errors in IWD estimation. Incorporating spatiotemporally varying crop coefficients and *IWUEC* values is therefore essential for reliable basin-scale IWD assessment.

https://doi.org/10.5194/essd-2026-128
Preprint. Discussion started: 9 March 2026

Open Access Earth System Science Data Discussions

Table 1. Comparison of representative CWR/IWD datasets across spatial scales

Dataset/ Study	Spatial extent	Temporal coverage	Spatial resolution	Crop types	Cropland data & uncertainty
Wada et al. (2013)	Global	1979-2010	0.5° (~50 km)	Not differentiated	Model-based; No validation
Hung et al. (2025)	Global	2000, 2005, 2010, 2015	60 m	Not differentiated	Single product; No validation
AQUASTAT (Frenken and Gillet, 2012)	Global	Static	Country	>30 classes	Not applicable
Fan et al. (2025)	China	2000-2018	~9 km	10 classes (rice, winter wheat, spring wheat, summer maize, spring maize, soybean, cotton, peanut, tubers, and beet)	Single product; No validation
Liu et al. (2009)	China	1970-2000	Regional	6 classes (winter wheat, spring wheat, summer maize, spring maize, cotton, rice)	Not applicable
Zhao et al. (2025)	China	2000-2020	3 km	5 classes (winter wheat, spring wheat, summer maize, spring maize, rice)	Single product; No validation
Liu et al. (2022)	YRB	1974-2017	Station-based	4 classes (spring wheat, winter wheat, spring maize and summer maize)	Not applicable
Niu et al. (2022)	YRB	1970-2005	Prefecture-level	5 classes (winter wheat, spring wheat, summer maize, spring maize, rice)	Single product; No validation
Hou et al. (2025)	YRB	2001-2018	10 km	5 classes (winter wheat, spring wheat, summer maize, spring maize, rice)	Single product; No validation
This study	YRB	2000-2020	500 m	25 classes	Eight products; Accuracy comparison

To address these limitations, this study develops a high-resolution (500 m) IWD dataset for the YRB covering 25 crop types from 2000 to 2020. The specific objectives are to: (1) systematically evaluate

https://doi.org/10.5194/essd-2026-128
Preprint. Discussion started: 9 March 2026

multiple state-of-the-art cropland datasets using county-level statistical data to identify the optimal product for the YRB; (2) estimate CWR and IWD with spatially explicit crop parameters and spatiotemporally dynamic IWUEC; (3) quantify the IWD underestimation resulting from incomplete crop coverage and characterize its spatiotemporal patterns across the basin. This dataset provides the first comprehensive, high-resolution IWD estimates incorporating nearly complete crop coverage for a major river basin. To serve both theoretical assessment and operational management needs, CWR and IWD are estimated under two scenarios: one based on total sown area (reflecting the full agricultural water gap) and one adjusted for actual irrigated area (reflecting practical irrigation demand).

2 Study area and data

2.1 Study area

The YRB, located in northern China (95°53'–119°05'E, 32°10'–41°50'N), covers approximately 795,000 km^2 and spans nine provinces (Fig. 1). The basin is conventionally divided into three reaches, namely the upper reach (from the river source to Toudaoguai hydrological station, 428,000 km^2), the middle reach (from Toudaoguai to Huayuankou station, 344,000 km^2), and the lower reach (below Huayuankou station, 23,000 km^2) (Liu et al., 2012; Yang et al., 2010). The YRB exhibits pronounced climate gradients, transitioning from semi-humid conditions in the southeast to semi-arid and arid zones in the northwest. Mean annual temperature ranges from -4°C to 14°C, generally decreasing from south to north and from east to west.

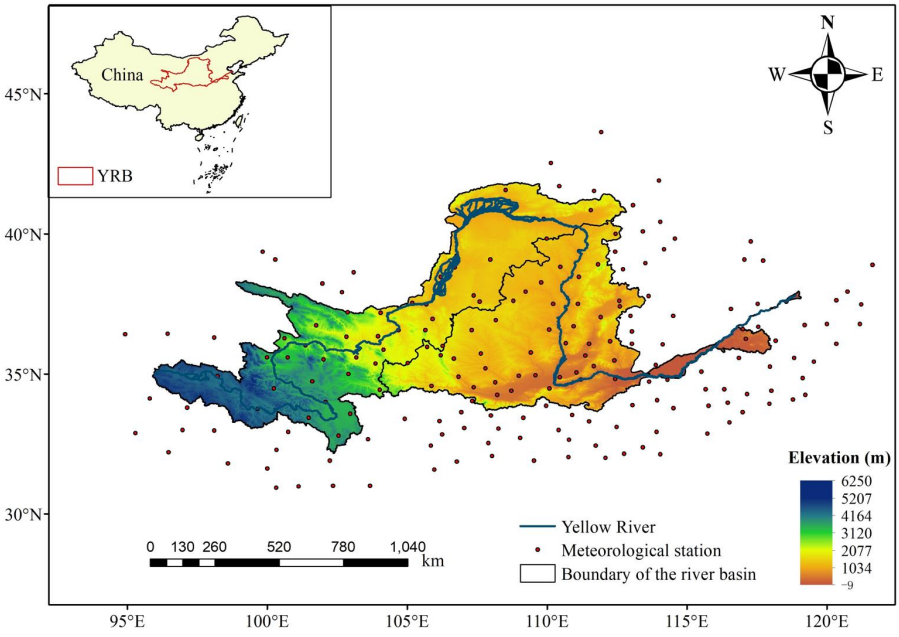

Figure 1: Overview of the study area.

https://doi.org/10.5194/essd-2026-128
Preprint. Discussion started: 9 March 2026

The YRB is a critical agricultural region in China, with 15.5 million hectares of cropland producing 35.4% of the national grain output (Hu et al., 2012). The basin supports complex and diverse cropping systems, with major grain crops (wheat and maize) coexisting with extensive cultivation of cotton, soybean, rice, oil crops, vegetables, and other economic crops. Agricultural irrigation annually consumes 67% of total water use in the basin. Despite improvements in irrigation efficiency through water-saving technologies, the tension between agricultural water demand and limited water availability remains a critical challenge for regional food security.

2.2 Data

2.2.1 Cropland datasets

This study collected eight remote sensing-based land cover or cropland datasets for comparative evaluation (Table 2). These datasets vary in spatial resolution (30 m to 5 km), temporal coverage, geographic extent (China or global), and classification approaches. CACD is a 30 m resolution annual cropland dataset for China (1986–2021), produced using Landsat imagery and random forest classification (Tu et al., 2024). CLCD provides 30 m annual land cover maps for China (1990–2019) with nine land cover classes (Yang and Huang, 2021). ESA-CCI is a global 300 m annual land cover product (1992–2020) derived from multiple satellite sources using the GlobCover classification chain (Esa, 2017). MCD12Q1 offers global 500 m land cover maps (2001–2022) based on MODIS data using decision tree and neural network algorithms (Friedl and Sulla-Menashe, 2022). MCID is a 500 m cropland dataset for China (2000–2015) derived from MOD09A1 products (Yan et al., 2019). GLASS-GLC provides global 5 km land cover maps (1982–2015) with seven classes (Liu et al., 2020). GLAD provides global 30 m cropland maps using Landsat data and bagged decision tree classification (Potapov et al., 2022). CLUD-A offers 30 m land cover maps for China (1980–2015) by integrating MODIS, GIMMS, and Landsat data (Xu et al., 2020).

Table 2. Summary of the eight cropland datasets

Dataset	Temporal coverage	Resolution	Extent	Primary data source
CACD	1986-2021	30m	China	Landsat
CLCD	1990-2019	30m	China	MODIS and Landsat
ESA-CCI	1992-2020	300m	Global	AVHRR, MERIS, and PROBA-V
MCD12Q1	2001-2022	500m	Global	MODIS Terra+Aqua
MCID	2000-2015	500m	China	MODIS
GLASS-GLC	1982-2015	5km	Global	MODIS and GLASS products
GLAD	2000-2019	30m	Global	Landsat
CLUD-A	1980-2015	30m	China	AVHRR, MODIS, and Landsat

https://doi.org/10.5194/essd-2026-128
Preprint. Discussion started: 9 March 2026

2.2.2 Meteorological data

Daily meteorological observations from 199 China Meteorological Administration stations within and surrounding the YRB were obtained for the period 2000–2020 (Fig. 1). Variables include precipitation, mean/maximum/minimum air temperature, wind speed, sunshine duration, and relative humidity. For stations with missing data, gaps of ≤5 consecutive days were filled using linear interpolation, while longer gaps were supplemented using gridded data extracted from the CN05.1 dataset (Wu et al., 2017).

2.2.3 Crop parameters and agricultural statistics

(1) Sown area and cropland area data

Crop-specific sown area data were compiled from statistical yearbooks of nine provinces within the YRB, including Shanxi, Inner Mongolia, Shaanxi, and others. We prioritized data collection at the county level to maximize spatial resolution. However, when county-level data were unavailable or had significant gaps, we substituted with prefecture-level statistics for the corresponding administrative region. Ultimately, sown area information for 25 crop types was compiled across 170 administrative units comprising both counties and prefectures (Fig. A1). The compiled sown area data are summarized in Table 3, which presents annual sown area for each crop type of the YRB. For cropland dataset validation, county-level cropland area data from 2001 to 2015 were utilized, as this period represents the overlapping temporal coverage of all eight candidate remote sensing datasets evaluated in this study. For IWD estimation, crop-specific sown area data covering the full study period (2000-2020) were used to calculate CWR and IWD for 25 crop types.

Table 3. Annual sown area of the 25 crop types in the Yellow River Basin during the 2000-2020 period.

Year	Spring maize	Summer maize	Spring wheat	Winter wheat	Beet	Coarse cereals	Flax	Fruits	Green fodder	Millet	Melons and gourds	Oil crops	Rice	Peanut	Tubers	Potato	Rapeseed	Sesame	Sorghum	Spring soybean	Summer soybean	Sunflower seed	Sweet potato	Cotton	Vegetables
	Unit: 10^4 km^2																								
2000	1.13	2.26	1.20	4.60	0.02	0.08	0.04	0.18	0.10	0.18	0.12	0.67	0.20	0.43	0.83	0.43	0.07	0.02	0.05	0.11	0.41	0.24	0.14	0.25	1.10
2001	1.17	2.28	1.12	4.40	0.02	0.08	0.02	0.18	0.09	0.16	0.13	0.70	0.19	0.43	0.83	0.41	0.06	0.01	0.04	0.12	0.38	0.23	0.12	0.33	1.15
2002	1.20	2.35	1.07	4.35	0.02	0.07	0.03	0.20	0.14	0.16	0.13	0.70	0.19	0.42	0.83	0.38	0.08	0.01	0.04	0.12	0.38	0.24	0.12	0.31	1.27
2003	1.27	2.35	1.00	4.19	0.02	0.06	0.03	0.22	0.15	0.15	0.14	0.73	0.17	0.42	0.79	0.39	0.09	0.01	0.04	0.11	0.36	0.23	0.11	0.40	1.35
2004	1.34	2.57	0.97	3.95	0.02	0.05	0.02	0.24	0.14	0.14	0.12	0.71	0.17	0.41	0.78	0.36	0.11	0.01	0.03	0.12	0.35	0.21	0.10	0.47	1.40
2005	1.39	2.68	0.99	4.18	0.02	0.07	0.02	0.25	0.16	0.13	0.14	0.66	0.19	0.40	0.78	0.39	0.11	0.01	0.03	0.12	0.35	0.21	0.10	0.43	1.43
2006	1.40	2.79	0.97	4.21	0.02	0.07	0.02	0.28	0.15	0.14	0.16	0.63	0.20	0.38	0.85	0.40	0.10	0.01	0.03	0.12	0.34	0.18	0.10	0.46	1.45
2007	1.49	2.90	0.94	4.20	0.02	0.07	0.01	0.32	0.17	0.14	0.17	0.59	0.21	0.38	0.87	0.39	0.07	0.01	0.03	0.11	0.32	0.18	0.07	0.49	1.46
2008	1.60	3.02	0.96	4.15	0.02	0.07	0.03	0.32	0.15	0.12	0.18	0.65	0.21	0.39	0.89	0.39	0.09	0.01	0.02	0.11	0.32	0.22	0.07	0.46	1.46
2009	1.76	3.21	1.02	4.22	0.01	0.07	0.03	0.32	0.14	0.13	0.18	0.67	0.20	0.39	0.88	0.41	0.09	0.01	0.02	0.11	0.31	0.23	0.07	0.42	1.54
2010	1.93	3.32	0.97	4.24	0.01	0.08	0.03	0.32	0.13	0.13	0.18	0.66	0.21	0.39	0.88	0.42	0.08	0.01	0.03	0.10	0.31	0.27	0.07	0.38	1.58
2011	1.96	3.30	0.95	4.20	0.01	0.09	0.02	0.33	0.12	0.12	0.19	0.64	0.20	0.39	0.87	0.41	0.08	0.01	0.02	0.09	0.30	0.29	0.07	0.36	1.63
2012	2.06	3.39	0.96	4.15	0.01	0.11	0.03	0.34	0.13	0.11	0.19	0.62	0.20	0.38	0.87	0.38	0.09	0.01	0.02	0.08	0.29	0.28	0.08	0.31	1.66
2013	2.20	3.48	0.90	4.06	0.01	0.10	0.02	0.34	0.12	0.11	0.19	0.61	0.19	0.37	0.86	0.37	0.10	0.01	0.02	0.09	0.27	0.29	0.07	0.27	1.67
2014	2.32	3.49	0.86	4.02	0.01	0.12	0.02	0.34	0.14	0.13	0.20	0.59	0.19	0.37	0.80	0.35	0.11	0.01	0.02	0.09	0.24	0.32	0.07	0.23	1.70
2015	2.40	3.50	0.87	3.99	0.01	0.12	0.02	0.34	0.14	0.15	0.19	0.57	0.18	0.36	0.78	0.31	0.10	0.01	0.01	0.09	0.23	0.36	0.07	0.21	1.75
2016	2.31	3.51	0.86	3.96	0.01	0.12	0.02	0.34	0.14	0.15	0.19	0.56	0.16	0.34	0.80	0.31	0.11	0.01	0.02	0.09	0.20	0.42	0.07	0.15	1.75
2017	2.33	3.59	0.86	3.97	0.00	0.11	0.02	0.23	0.12	0.16	0.17	0.53	0.17	0.32	0.67	0.28	0.08	0.01	0.02	0.09	0.20	0.44	0.07	0.08	1.54
2018	2.48	3.56	0.85	3.93	0.01	0.11	0.01	0.24	0.12	0.15	0.17	0.52	0.18	0.33	0.66	0.26	0.06	0.01	0.06	0.10	0.20	0.40	0.06	0.07	1.49
2019	2.50	3.48	0.84	3.86	0.01	0.11	0.01	0.25	0.14	0.16	0.17	0.50	0.16	0.32	0.65	0.22	0.07	0.01	0.06	0.10	0.20	0.41	0.06	0.05	1.53
2020	2.58	3.53	0.79	3.80	0.01	0.11	0.01	0.25	0.15	0.17	0.17	0.49	0.14	0.32	0.64	0.20	0.06	0.01	0.06	0.10	0.19	0.42	0.07	0.05	1.56

https://doi.org/10.5194/essd-2026-128
Preprint. Discussion started: 9 March 2026

https://doi.org/10.5194/essd-2026-128
Preprint. Discussion started: 9 March 2026

(2) Crop coefficients (K_c)

K_c values for 25 crop types were primarily derived from Duan et al. (2004), who calibrated FAO-56 reference values using local climate and soil data at multiple representative stations across northern China. We compiled K_c values from 45 observation stations (Fig. A2) for 20 crop types, covering the four standard growth stages, which include initial (Kc_ini), development, mid-season (Kc_mid), and late-season (Kc_end) (Table S1). Winter wheat, which includes an overwintering period, has an additional frozen stage coefficient (Kc_fro). For five crop categories lacking locally calibrated values (vegetables, oil crops, green fodder, rapeseed, and coarse cereals), K_c values were adopted directly from FAO-56 guidelines (Allen et al., 1998).

In addition, crop growth stage parameters, including planting dates and length of growth periods, were obtained from previous studies in the YRB (Liu et al., 2022) and National Earth System Science Data Center (2023) for major crops (e.g., spring maize, spring wheat, cotton, spring soybean, rice), and supplemented by the FAO AQUASTAT database (2024) and Siebert and Döll (2008) for other crops.

2.2.4 Irrigation water use efficiency coefficients (*IWUEC*)

Provincial annual *IWUEC* values were compiled from the China Water-Saving Irrigation Network (2025). Unlike previous studies that either neglected *IWUEC* or applied static coefficients (typically 0.5-0.7) uniformly across the basin (Zha et al., 2025), this study incorporated *IWUEC* values that vary both spatially (by province) and temporally (annual values from 2000 to 2020), reflecting improvements in irrigation infrastructure and water-saving technologies over the study period. For years prior to 2009 when official statistics were unavailable, *IWUEC* values were estimated using linear interpolation based on the temporal trend derived from the available period (2009-2020). Detailed values of *IWUEC* and related discussions on *IWUEC* uncertainties are provided in the supplementary Fig. A3 and Sect. 5.2, respectively.

3 Methods

The methodology comprises four main steps (Fig. 2). Since IWD estimation requires spatially explicit cropland distribution to allocate crop water consumption to specific locations, we first evaluated eight remote sensing cropland datasets to identify the optimal product for the YRB (Sect. 3.1). Meteorological and crop parameter data were then preprocessed and interpolated to a uniform 500-m grid (Sect. 3.2.1). CWR and IWD were subsequently calculated for 25 crop types using the FAO Penman-Monteith approach (Sect. 3.2.2). Finally, we analyzed the spatiotemporal patterns of IWD and quantified the underestimation resulting from incomplete crop coverage in previous studies (Sect. 3.3).

https://doi.org/10.5194/essd-2026-128
Preprint. Discussion started: 9 March 2026

Open Access Earth System Science Data Discussions

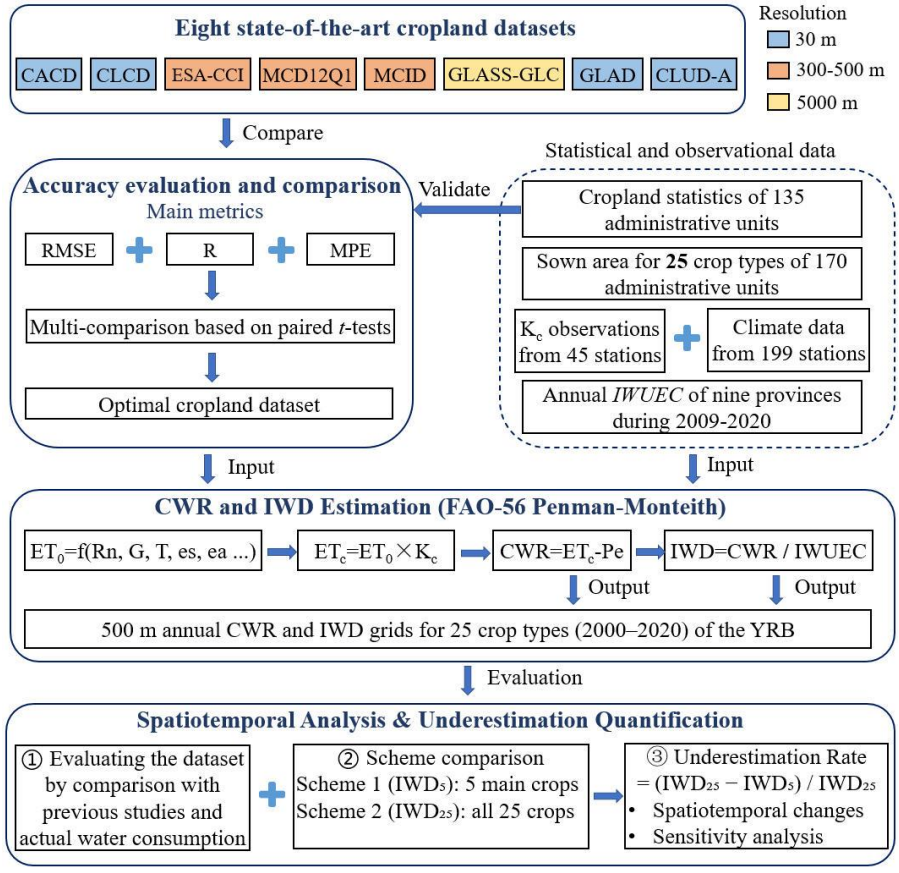

Figure 2: Flowchart of the methodology framework for CWR and IWD estimation in the Yellow River Basin. The color shading of cropland dataset names indicates their spatial resolution.

3.1 Cropland dataset evaluation and selection

Because existing cropland products show large discrepancies (Liu et al., 2025), we first evaluated eight datasets (Table 2) to identify the optimal product for the YRB. Cropland area from provincial statistical yearbooks (2001–2015) served as reference data. Among the 170 administrative units with compiled statistics, 135 units with relatively complete data series (i.e., missing data for no more than 6 years during the validation period) were selected for dataset evaluation to ensure reliability. Three complementary metrics were employed for evaluation, including root mean square error (RMSE), mean percentage error (MPE), and Pearson correlation coefficient (R).

RMSE measures the absolute deviation between remote sensing estimates and statistical reference data. MPE indicates systematic bias as a percentage of reference values. These metrics were calculated following equations (1)-(2):

$$RMSE = \sqrt{\sum_{i=1}^{N}(x_i - r_i)^2 / N} \quad (1)$$

https://doi.org/10.5194/essd-2026-128
Preprint. Discussion started: 9 March 2026

$$MPE = \left(\sum_{i=1}^{N}\left(\frac{x_i - r_i}{r_i}\right)/N\right) \times 100\% \quad (2)$$

where, x_i is the estimated cropland area from the remote sensing dataset, r_i is the corresponding reference value, N is the number of available years. RMSE and MPE are first computed for each administrative unit then averaged across the YRB.

R measures the spatial consistency between dataset estimates and reference data and is calculated following equation (3):

$$R = \frac{\sum_{i=1}^{C}(x_i - \bar{x}) \times (r_i - \bar{r})}{\sqrt{\sum_{i=1}^{C}(x_i - \bar{x})^2} \times \sqrt{\sum_{i=1}^{C}(r_i - \bar{r})^2}} \quad (3)$$

where, C is the number of administrative units. The higher the R value, the stronger the spatial consistency of the dataset in capturing cropland distribution. R was calculated annually and then averaged across all years.

To determine whether accuracy differences among datasets were statistically significant, we performed pairwise comparisons using paired *t*-tests across all county-year observations. The Holm-Bonferroni method was applied to control the family-wise error rate under multiple comparisons (Holm, 1979).

Cropland area was extracted by overlaying boundaries of administrative units with each dataset. The optimal dataset was selected based on minimizing RMSE, MPE close to zero, and maximizing R. The selected dataset was then used as the spatial basis for subsequent IWD estimation.

3.2 Crop water requirement and irrigation water demand estimation

3.2.1 Data preprocessing and spatial interpolation

(1) Meteorological data interpolation

Daily meteorological variables from 199 weather stations were interpolated to a 500-m grid using inverse distance weighting (IDW). Elevation-based temperature correction was applied with a lapse rate of -6.5 °C/km (Wang et al., 2021b).

(2) Crop coefficient spatialization

Crop coefficients (K_c) for 20 crop types with local observations were spatially interpolated to generate continuous 500-m resolution fields using IDW interpolation from stations within and around the YRB. For the remaining five crop categories lacking locally calibrated values (vegetables, oil crops, green fodder, rapeseed, and coarse cereals), spatially uniform K_c values were adopted from FAO-56 guidelines. Additionally, crop growth stage parameters, including planting dates and length of growth periods, were assigned as spatially constant values across the study area.

(3) Spatial allocation of crop-specific sown area

Crop-specific sown area from statistical yearbooks was spatially allocated to 500-m cropland pixels using the selected cropland dataset as the spatial reference. For each administrative unit, the sown area of each crop type was uniformly distributed across all cropland pixels within the county:

$$S_{i,j} = \frac{A_i}{N_c} \quad (4)$$

where, $S_{i,j}$ is the allocated sown area for crop i in pixel j, A_i is the total sown area of crop i in the administrative unit (from statistical yearbooks), and N_c is the number of cropland pixels within the

https://doi.org/10.5194/essd-2026-128
Preprint. Discussion started: 9 March 2026

administrative unit (from the selected remote sensing dataset). For administrative units intersected by the basin boundary, the allocation was first performed across the entire administrative unit, and then spatially clipped to retain only pixels within the YRB. This approach ensures spatial continuity while maintaining consistency between statistical totals and remote sensing-derived cropland distribution.

3.2.2 CWR and IWD estimation

CWR and IWD were estimated using the FAO-56 Penman-Monteith approach (Allen et al., 1998). The estimation procedure consists of four main components. First, reference evapotranspiration (ET_0) was calculated from daily meteorological variables including radiation, air temperature, wind speed, and humidity. Second, crop-specific evapotranspiration (ET_c) was derived by applying spatially heterogeneous crop coefficients (K_c) to ET_0. Third, CWR was computed as the difference between ET_c and effective precipitation (P_e) accumulated over the growing season. Finally, IWD was estimated by dividing CWR by IWUEC that accounts for water losses during conveyance and application. Detailed calculations for each component are described below.

ET_0 was calculated following equation (5):

$$ET_0 = \frac{0.408\Delta(R_n - G) + \gamma \frac{900}{T+273} U_2 (e_s - e_a)}{\Delta + \gamma(1 + 0.34U_2)} \quad (5)$$

where, R_n is the net radiation, estimated from sunshine duration and maximum/minimum air temperature following the procedures in FAO-56 (Allen et al., 1998); G is the soil heat flux (assumed negligible for daily calculations); T is the mean daily air temperature; e_s and e_a are saturation and actual water vapour pressure; Δ is the slope of saturated water vapour curve; γ is the psychrometric constant; U_2 is the wind speed at 2-m height. e_s and e_a were estimated based on air temperature and humidity.

ET_c was calculated as:

$$ET_c = K_c \times ET_0 \quad (6)$$

where, K_c is the spatially interpolated crop coefficient (Sect. 3.2.1). Growth stages were divided into initial, development, mid-season, and late-season stages for most crops, with an additional overwintering stage for winter wheat.

P_e was calculated following Döll and Siebert (2002) based on daily rainfall P_i:

$$P_e = \begin{cases} 4.17 + 0.1 \times P_i & P_i \geq 8.3\ mm/d \\ P_i \times \frac{4.17 - 0.2 \times P_i}{4.17} & P_i < 8.3\ mm/d \end{cases} \quad (7)$$

CWR, representing the net water requirement after accounting for effective precipitation (note that CWR as defined here corresponds to the "net irrigation water requirement" in some literature, rather than the total crop evapotranspiration sometimes denoted by the same abbreviation), was calculated as:

$$CWR = \frac{S \times (ET_c - P_e)}{1000} \quad (8)$$

where, S is the sown area of the corresponding crop type.

IWD was calculated as:

$$IWD = \frac{CWR}{IWUEC} \quad (9)$$

where, *IWUEC* is the irrigation water use efficiency coefficient.

https://doi.org/10.5194/essd-2026-128
Preprint. Discussion started: 9 March 2026

Open Access Earth System Science Data Discussions

Grid-level CWR and IWD values (in mm/yr) were converted to volumetric water demand (m^3/yr) by multiplying by pixel area. For area calculation, the WGS84 grid was projected to the Albers equal-area conic projection, yielding a near-uniform pixel size of approximately 442 × 442 m^2. The dataset is distributed in its native WGS84 geographic coordinate system. The resulting volumetric values were then aggregated to sub-basin and basin scales.

In addition to these sown area-based estimates, an actual irrigated area-based version was generated by masking with the CIrrMap250 annual irrigated cropland dataset (Zhang et al., 2024). The details are provided in Sect. 5.2(1).

3.3 Spatiotemporal analysis and underestimation quantification

Annual IWD was analyzed at multiple spatial scales, including 500-m pixels and sub-basins (upper, middle, and lower reaches), and the entire basin. Temporal trends over the 2000–2020 period were examined using linear regression, and spatial variations were characterized across the three reaches with distinct climate and agricultural conditions.

To quantify the systematic underestimation caused by incomplete crop coverage in previous studies, we compared IWD estimates from two schemes: Scheme 1 (Limited coverage) considers five major crops, including spring wheat, winter wheat, spring maize, summer maize, and rice, representing the typical approach in previous YRB studies (Chen et al., 2023; Liu et al., 2022; Zhao et al., 2025; Hou et al., 2025); Scheme 2 (Comprehensive coverage) considers all 25 crop types (Table 3). The underestimation rate (UR) was calculated as:

$$UR = \frac{IWD_{25} - IWD_5}{IWD_{25}} \times 100\% \quad (10)$$

where, IWD_{25} and IWD_5 are the IWD estimates from Schemes 2 and 1, respectively. Both the spatial heterogeneity (across sub-basins) and temporal dynamics (annual variations from 2000 to 2020) of underestimation were examined.

4 Results

4.1 Accuracy assessment of cropland datasets

The accuracy assessment results for eight cropland datasets reveal substantial differences among datasets across all three evaluation metrics (Fig. 3), highlighting the importance of dataset selection for IWD estimation.

https://doi.org/10.5194/essd-2026-128
Preprint. Discussion started: 9 March 2026

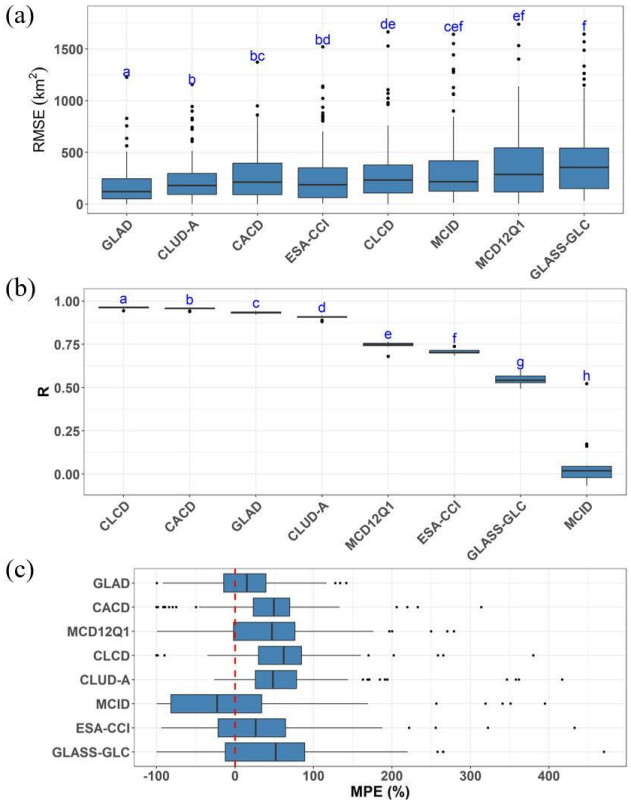

Figure 3: Accuracy assessment of eight cropland datasets against statistical data. (a) Root mean square error (RMSE) for each dataset, with products ordered by ascending mean RMSE. (b) Pearson correlation coefficient (R) for each dataset, with products ordered by descending mean R. (c) Mean percentage error (MPE) for each dataset, with products ordered by descending absolute MPE values. The red dashed line in (c) indicates MPE = 0. Different lowercase letters above the boxplots indicate statistically significant differences among datasets based on paired *t*-tests with Holm-Bonferroni correction ($P < 0.05$), while datasets sharing the same letter are not significantly different. Boxplots represent county-level values across 2001–2015, with the horizontal line indicating the median, box edges representing the 25th and 75th percentiles, and whiskers extending to 1.5 times the interquartile range.

Among the evaluated datasets, GLAD demonstrated the best overall performance, with the lowest mean RMSE (287.31 km^2), the lowest absolute mean MPE (15.00%), and a high mean spatial correlation coefficient (R = 0.93). Notably, multi-comparison results indicate that GLAD's county-level RMSE was statistically significantly lower ($P < 0.05$) than all other seven products (Fig. 3a). Although GLAD's county-level R was statistically significantly lower ($P < 0.05$) than CLCD and CACD (Fig. 3b), the mean difference was relatively minor (0.03). CACD also performed well, with strong spatial consistency (mean R = 0.96) but presented notable overestimation (mean MPE = 45.19%) and higher mean RMSE (501.81 km^2). CLCD and CLUD-A showed similar patterns, with high mean R values (0.96 and 0.91) but substantial overestimation (mean MPE = 66.65% and 90.02%, respectively).

In contrast, several global and coarse-resolution datasets presented poor performance in the YRB.

https://doi.org/10.5194/essd-2026-128
Preprint. Discussion started: 9 March 2026

ESA-CCI and GLASS-GLC showed much higher overestimation (Fig. 3c), indicating severe systematic bias in cropland area estimation. MCD12Q1, despite its moderate RMSE (691.56 km^2), showed limited spatial consistency (mean R = 0.75) and substantial overestimation (mean MPE = 59.68%).

Thus, we selected GLAD for subsequent analysis because it had the lowest RMSE, the smallest systematic bias, and strong spatial correlation with statistical data.

4.2 Cropping structure of the YRB

A total of 25 crop types were recorded in the YRB over the 2000–2020 period (Fig. 4). The three dominant crops by sown area (21-year average) were winter wheat (41,000 km^2), summer maize (31,000 km^2), and spring maize (18,000 km^2), collectively accounting for approximately 57% of total sown area. All other crop types individually occupied less than 15,000 km^2, including spring wheat, vegetables, oil crops, cotton, millet, potatoes, fruits, and various other crops (Fig. 4b).

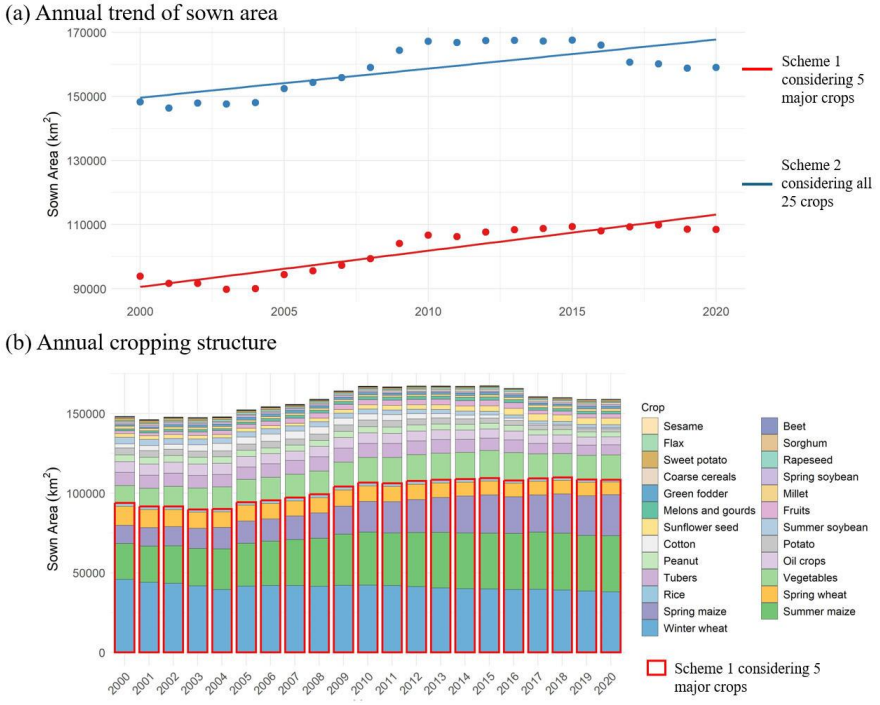

Figure 4: Annual sown area changes and cropping structure in the YRB (2000–2020).

The total sown area in the YRB presented a significant increasing trend of 900 km^2/yr over the study period ($P < 0.001$), rising from approximately 148,000 km^2 in 2000 to 168,000 km^2 in 2015 before slightly declining to 159,000 km^2 in 2020 (Fig. 4a). Similarly, the sown area of the five major crops (spring wheat, winter wheat, spring maize, summer maize, and rice) showed a significant increasing trend of 1,100 km^2/yr ($P < 0.001$).

Clear differences existed between the two schemes in terms of total sown area coverage (Fig. 4b). The multi-year average sown area under Scheme 2 (all 25 crops) was approximately 159,000 km^2,

https://doi.org/10.5194/essd-2026-128
Preprint. Discussion started: 9 March 2026

compared to 102,000 km^2 under Scheme 1 (five major crops only), indicating that Scheme 1 covered only 64.2% of the total sown area. This implies that studies considering only major crops would systematically exclude 35.8% of the cultivated area from water consumption estimation, potentially leading to considerable underestimation of basin-scale irrigation water demand.

4.3 Spatiotemporal changes of CWR

The high-resolution cropland data combined with county-level allocation of 25 crop types enabled CWR estimation with rich spatial detail (Fig. 5a). The multi-year average annual CWR for the entire YRB was 548.3 × 10^8 m^3 under Scheme 2. The middle reach contributed the largest share (306.7 × 10^8 m^3, 55.9%), followed by the upper reach (164.4 × 10^8 m^3, 30.0%) and the lower reach (77.2 × 10^8 m^3, 14.1%) (Fig. 5b).

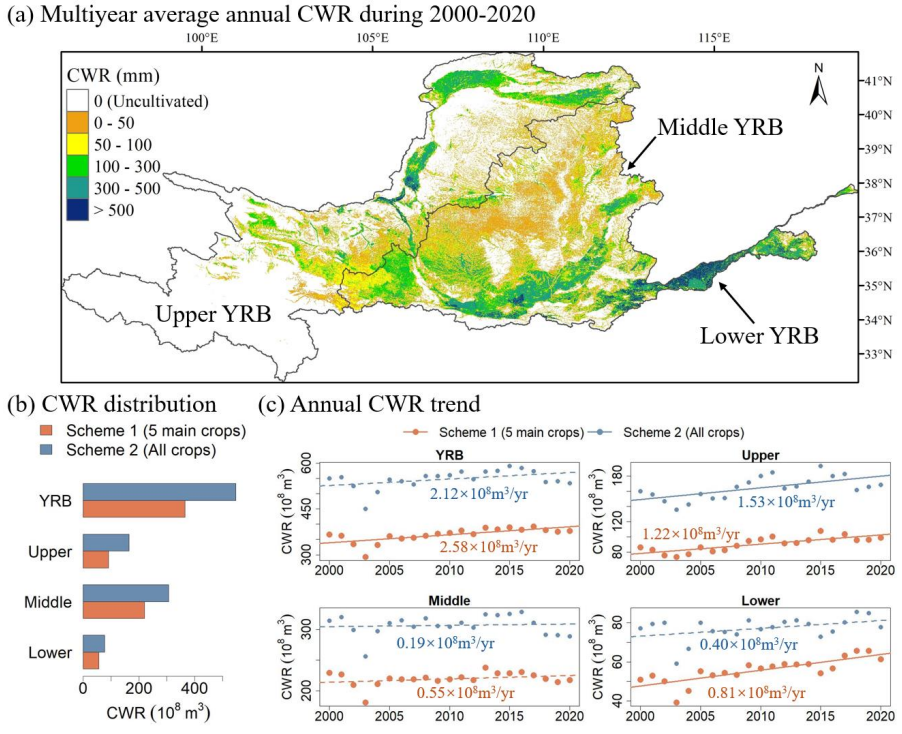

Figure 5: Spatiotemporal variations of CWR in the Yellow River Basin during 2000-2020. (a) Spatial distribution of multi-year average annual CWR; (b) Comparison of multi-year average CWR between Scheme 1 (5 main crops) and Scheme 2 (all 25 crops) across different sub-basins; (c) Interannual variations of CWR for each sub-basin. In panel (c), solid lines indicate statistically significant trends (P < 0.05), while dashed lines indicate non-significant trends.

Considering only five major crops (Scheme 1) resulted in substantial underestimation of CWR across all spatial scales. For the entire YRB, CWR under Scheme 1 was 365.9 × 10^8 m^3, representing a

https://doi.org/10.5194/essd-2026-128
Preprint. Discussion started: 9 March 2026

Open Access Earth System Science Data Discussions

33.3% underestimation compared to Scheme 2. This underestimation presented pronounced spatial heterogeneity. The upper reach showed the largest underestimation (44.9%), while the middle and lower reaches showed relatively lower but still considerable underestimation (28.4% and 27.9%, respectively) (Fig. 5b).

Both schemes showed increasing trends in CWR over the 2000–2020 period, but with notably different magnitudes (Fig. 5c). For the entire YRB, Scheme 1 presented a statistically significant increasing trend of 2.58 × 10^8 m^3/yr ($P < 0.05$), whereas Scheme 2 showed a weaker and non-significant trend of 2.12 × 10^8 m^3/yr. Similar patterns were observed in the lower reach, where Scheme 1 showed a significant increase of 0.81 × 10^8 m^3/yr ($P < 0.05$) compared to a non-significant increase of 0.40 × 10^8 m^3/yr under Scheme 2. Although both schemes presented statistically significant increasing trends in the upper and middle reaches, the magnitude of increase differed substantially. For instance, in the middle reach, the increasing rate under Scheme 1 (0.55 × 10^8 m^3/yr) was nearly three times that of Scheme 2 (0.19 × 10^8 m^3/yr).

4.4 Spatiotemporal changes of IWD

The spatial pattern of IWD was similar to that of CWR, as the two variables differ only by the *IWUEC* factor (Fig. 6a). The multi-year average annual IWD for the entire YRB was 1086.8 × 10^8 m^3 under Scheme 2. The middle reach contributed the largest share (590.5 × 10^8 m^3, 54.3%), followed by the upper reach (359.6 × 10^8 m^3, 33.1%) and the lower reach (136.7 × 10^8 m^3, 12.6%) (Fig. 6b).

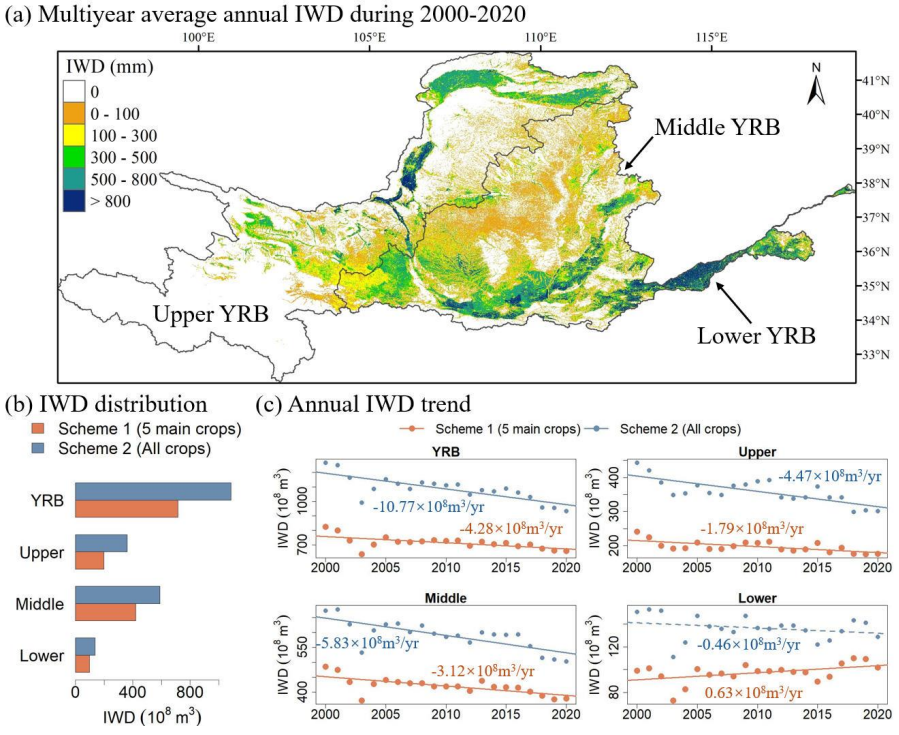

https://doi.org/10.5194/essd-2026-128
Preprint. Discussion started: 9 March 2026

Figure 6: Spatiotemporal variations of IWD in the Yellow River Basin during 2000-2020. (a) Spatial distribution of multi-year average annual IWD; (b) Comparison of multi-year average IWD between Scheme 1 (5 main crops) and Scheme 2 (all 25 crops) across different sub-basins; (c) Interannual variations of IWD for each sub-basin. In panel (c), solid lines indicate statistically significant trends ($P < 0.05$), while dashed lines indicate non-significant trends.

Consistent with the CWR results, considering only five major crops (Scheme 1) led to substantial underestimation of IWD. For the entire YRB, IWD under Scheme 1 was 714.8 × 10^8 m^3, representing a 34.2% underestimation compared to Scheme 2. The spatial heterogeneity of underestimation was also similar to CWR. The upper reach presented the largest underestimation (45.1%), while the middle and lower reaches showed underestimation of 28.9% and 28.8%, respectively (Fig. 6b).

In contrast to the increasing trends observed for CWR, IWD presented decreasing trends across most regions over the 2000–2020 period (Fig. 6c), primarily attributable to improvements in *IWUEC* during this period (discussed further in Sect. 5.3). The magnitude of IWD trends differed substantially between the two schemes. For the entire YRB, Scheme 2 showed a stronger decreasing trend (-10.77 × 10^8 m^3/yr, $P < 0.05$) compared to Scheme 1 (-4.28 × 10^8 m^3/yr, $P < 0.05$). Similar patterns were observed in the upper and middle reaches.

The most striking result was that the two schemes yielded opposite trend directions in the lower reach. Scheme 2 presented a non-significant decreasing trend (-0.46 × 10^8 m^3/yr), whereas Scheme 1 showed a significant increasing trend (0.63 × 10^8 m^3/yr, $P < 0.05$). This divergence highlights that incomplete crop coverage may not only underestimate the absolute magnitude of IWD but also lead to fundamentally different conclusions regarding temporal changes of IWD.

5 Discussions

5.1 Evaluation of the dataset and comparison with previous estimates

Direct validation of IWD estimates is challenging for two primary reasons. First, IWD represents a theoretical water demand based on crop physiological requirements and climate conditions (Frenken and Gillet, 2012), fundamentally different from actual water use statistics that are influenced by water availability constraints, management practices, and socioeconomic factors (Archer et al., 2010). For instance, recent studies have demonstrated that significant spatiotemporal mismatches exist between IWD and actual water allocation in the YRB (Hou et al., 2025). Second, most previous IWD studies at the basin scale have either neglected *IWUEC* or applied spatially uniform and temporally static *IWUEC* values (Zha et al., 2025; Fu et al., 2022; Liu et al., 2022), making it difficult to establish comparable benchmarks for validation.

Given these constraints, we first evaluated the reliability of our dataset by comparing key intermediate variables (ET_0 and CWR) with independent estimates from previous studies, then examined the consistency of IWD temporal trends with observed changes in actual irrigation water use.

For ET_0, our calculated multi-year average annual total for the YRB (2000–2020) was 1100.96 mm. This value falls within the range of 950–1150 mm reported by Wang et al. (2012) for 1957–2008 and is

https://doi.org/10.5194/essd-2026-128
Preprint. Discussion started: 9 March 2026

slightly lower than the approximately 1200 mm estimated by Liu and Yang (2010) for 1961–2006. Given that Liu and Yang (2010) also identified a declining trend in ET_0 over their study period, the slightly lower value in our more recent study period (2000–2020) is consistent with this temporal pattern, supporting the reliability of our ET_0 calculations.

For CWR, Peng et al. (2017) reported a mean annual net irrigation water requirement (equivalent to CWR in this study) of 271.93 × 10^8 m^3 for five major irrigation districts in the YRB during 2000–2010, considering all crop types including both grain and economic crops. These five districts account for approximately 52% of the total irrigated area in the YRB. Our estimate for the entire basin during the same period was 534.80 × 10^8 m^3, which is proportionally consistent with their results when accounting for the spatial coverage difference, further supporting the reliability of our CWR estimates.

For IWD, direct comparison with actual water use statistics requires careful interpretation. The multi-year average IWD based on total sown area (1086.8 × 10^8 m^3) substantially exceeds reported actual agricultural water consumption in the YRB, which was approximately 350–400 × 10^8 m^3 (Peng et al., 2021). This discrepancy is expected and arises from two sources. First, our sown area-based IWD covers all cropland including rainfed areas where irrigation is not applied. When restricted to actual irrigated area, IWD decreases to 508.4 × 10^8 m^3 (see Sect. 5.2(1)). Second, even on irrigated land, actual water delivery is constrained by water availability, infrastructure capacity, and allocation policies, so crops frequently receive less water than their theoretical demand. Peng et al. (2021) estimated that approximately 3.3 × 10^4 km^2 of irrigated cropland in the YRB (~20% of total sown area) was insufficiently irrigated or received no effective irrigation. Accounting for this deficit, the effective irrigation demand implied by their consumption estimate would be roughly 480 × 10^8 m^3, broadly consistent with our irrigated area-adjusted IWD (508.4 × 10^8 m^3). In addition, while the absolute magnitude of IWD thus cannot serve as a direct estimate of actual water consumption, temporal trends in IWD would be expected to reflect observed changes in actual water use. Indeed, the decreasing trend of IWD identified in this study is consistent with observed reductions in actual agricultural water use at multiple spatial scales. Zhu (2025) documented a declining trend in actual irrigation water consumption across the nine provinces encompassing the YRB during 2000–2023, and similar decreasing trends have been reported for Ningxia (Du et al., 2026) and Henan (Lu et al., 2017) provinces. This consistency across multiple independent studies provides indirect but important support for the reliability of our IWD estimates. Users should select the sown area-based version for assessing total agricultural water gaps and vulnerability, or the irrigated area-based version for operational water management, as discussed in Sect. 5.2(1).

While our ET_0, CWR and IWD estimates show good consistency with previous studies, this dataset advances beyond existing products in several important aspects. The comprehensive coverage of 25 crop types addresses a critical gap in previous studies that typically considered only 3–6 major crops, thereby reducing the significant underestimation of basin-scale water demand (Figs. 5b and 6b). The high spatial resolution of 500 m enables finer representation of heterogeneity in cropland distribution and irrigation requirements, which is essential for local water management planning (Figs. 5a and 6a). Most importantly, the incorporation of spatiotemporally dynamic *IWUEC* values provides more realistic IWD estimates that account for water losses during conveyance and application, losses that are often neglected in

https://doi.org/10.5194/essd-2026-128
Preprint. Discussion started: 9 March 2026

previous basin-scale studies where CWR is directly used as IWD. The importance of incorporating spatiotemporally dynamic *IWUEC* values is further discussed in Sect. 5.3.

5.2 Uncertainty and limitations

(1) Actual irrigated area

A key distinction exists between cropland area and actually irrigated area. CWR based on total cropland represents the theoretical water deficit across all cultivated land, including rainfed areas where irrigation is not applied. This full agricultural water gap is essential for irrigation infrastructure planning, agricultural potential assessment, and climate adaptation studies (Chai et al., 2016).

In contrast, CWR and IWD estimates based on actual irrigated area represent the water demand that is addressed through irrigation systems. Not all cropland in the YRB receives irrigation, particularly in areas where irrigation infrastructure is limited or economically unfeasible. To quantify this uncertainty, we applied the CIrrMap250 dataset (Zhang et al., 2024), which provides annual maps of China's irrigated cropland at 250-m resolution from 2000 to 2020 derived through multisource data integration. By masking our 500-m CWR and IWD grids with the annually varying irrigated area from CIrrMap250, we generated an alternative set of estimates (Fig. 7). The results reveal substantial differences. When considering actual irrigated area, multi-year average CWR decreased from 548.3×10^8 m^3 to 258.6×10^8 m^3 (a reduction of 52.8%), and IWD decreased from 1086.8×10^8 m^3 to 508.4×10^8 m^3 (a reduction of 53.2%). The difference between these two estimates (approximately 290×10^8 m^3 for CWR) represents the unmet water demand on rainfed cropland, which could be a critical indicator of agricultural vulnerability and potential for irrigation expansion.

https://doi.org/10.5194/essd-2026-128
Preprint. Discussion started: 9 March 2026

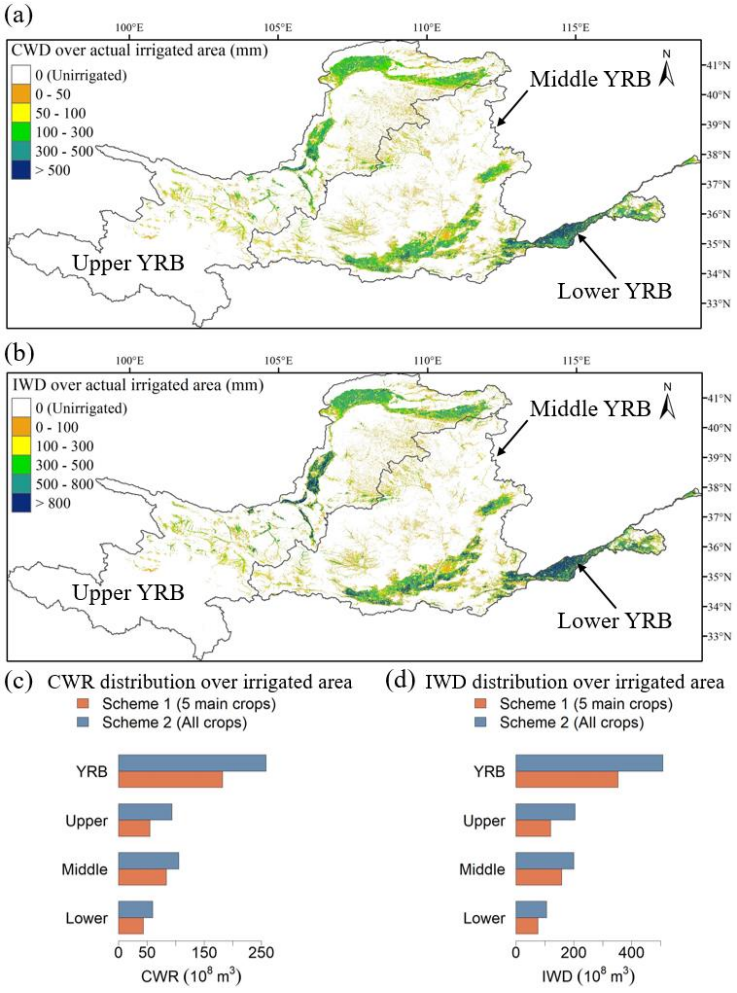

Figure 7: CWR and IWD estimates considering actual irrigated area in the Yellow River Basin. (a) Spatial distribution of multi-year average CWR over actual irrigated area; (b) Spatial distribution of multi-year average IWD over actual irrigated area; (c) Comparison of multi-year average CWR between Scheme 1 (5 main crops) and Scheme 2 (all 25 crops) across different sub-basins; (d) Comparison of multi-year average IWD between Scheme 1 (5 main crops) and Scheme 2 (all 25 crops) across different sub-basins. Unirrigated areas (including the cropland and non-cropland areas) are shown in white in panels (a) and (b).

Importantly, while accounting for actual irrigated area substantially reduces the absolute magnitude of CWR and IWD, our core finding regarding the underestimation caused by incomplete crop coverage remains robust. When considering actual irrigated area, the underestimation of CWR from using only five major crops (Scheme 1) was 29.7% for the entire YRB (Fig. 7c), compared to 33.3% based on total cropland area (Fig. 5b). The spatial pattern of underestimation remained consistent, with the upper reach

https://doi.org/10.5194/essd-2026-128
Preprint. Discussion started: 9 March 2026

exhibiting the largest underestimation (41.2% versus 44.9% previously). Similarly, the underestimation of IWD decreased slightly from 34.2% (Fig. 6c) to 30.5% (Fig. 7d) at the basin scale, while the upper reach continued to show the highest underestimation (41.3% versus 45.1% previously). These results demonstrate that regardless of whether actual irrigated area is considered, studies relying solely on major crops would systematically underestimate basin-scale water demand by approximately 30%, reinforcing the necessity of comprehensive crop coverage in regional IWD assessment.

This study provides both versions of the dataset to serve different research and management needs: (i) CWR and IWD based on total cropland area for assessing theoretical water demand and agricultural water gaps, and (ii) CWR and IWD adjusted for actual irrigated area for operational water management applications. Furthermore, users with access to higher-accuracy local irrigation maps can readily apply their own data to our gridded products, thereby refining estimates for specific regions of interest.

(2) *IWUEC*

The *IWUEC* values employed in this study were derived from official statistics. While these official statistics represent the most authoritative data source available for China, two primary uncertainties should be noted.

First, the provincial-scale *IWUEC* values cannot capture sub-provincial spatial heterogeneity in irrigation efficiency. In reality, *IWUEC* varies considerably within provinces due to differences in irrigation infrastructure (e.g., canal lining, drip irrigation adoption), crop types, soil properties, and local management practices (Jägermeyr et al., 2015; Du et al., 2026; Fu et al., 2022). By applying uniform *IWUEC* values across each province, our IWD estimates may overestimate water demand in areas with advanced irrigation systems while underestimating demand in less developed areas. Future studies incorporating sub-provincial or irrigation district-level efficiency data would further improve the spatial accuracy of IWD estimation.

Second, official *IWUEC* statistics were only available from 2009 onward, necessitating estimation for the 2000–2008 period through temporal extrapolation. We employed linear regression based on the 2009–2020 time series to hindcast *IWUEC* values for each province. The reliability of this extrapolation is supported by the strong linear relationships observed across all nine provinces encompassing the YRB, with coefficients of determination (R^2) ranging from 0.879 (Shandong) to 0.993 (Sichuan) (Fig. A3b-j). These high R^2 values indicate that *IWUEC* improvements followed consistent linear trajectories during the 2009–2020 period, likely driven by sustained national policies promoting water-saving irrigation technologies. The assumption that similar linear trends prevailed during 2000–2008 could be reasonable given that China's agricultural water-saving initiatives were already underway during this period (Mingzhong, 2000; Fu et al., 2022). Nevertheless, the extrapolated values for earlier years inevitably carry greater uncertainty than the directly reported values for 2009–2020.

Despite these limitations, the use of spatiotemporally dynamic *IWUEC* values is a methodological improvement over previous studies in the YRB that ignored *IWUEC* altogether or applied spatially uniform or temporally static coefficients (Liu et al., 2022; Niu et al., 2022). Our approach, while imperfect, better reflects the reality that irrigation efficiency has improved substantially over the past two decades and varies across provinces with different levels of agricultural development.

(3) Other sources of uncertainty

https://doi.org/10.5194/essd-2026-128
Preprint. Discussion started: 9 March 2026

Several additional factors contribute to uncertainty in CWR and IWD estimation, though their impacts are expected to be secondary compared to the factors discussed above.

The K_c values for 20 crop types were derived from 45 observation stations across northern China and spatially interpolated using inverse distance weighting. While this approach captures regional variations in crop water consumption characteristics, interpolation errors may occur in areas distant from observation stations. Additionally, K_c values for five crop categories (vegetables, oil crops, green fodder, rapeseed, and coarse cereals) were adopted directly from FAO-56 guidelines (Allen et al., 1998) due to the lack of locally calibrated values. Although this is a common practice in regional water use studies (Fan et al., 2025), these FAO reference values may not fully represent crop water use characteristics under the semi-arid continental climate conditions prevalent in much of the YRB. Similar uncertainties exist for crop calendar parameters, as planting dates and growth stage lengths derived from literature and FAO AQUASTAT do not capture interannual variability from climate and farmer decisions (Alimagham et al., 2024), nor spatial heterogeneity across elevations and latitudes (Mkuhlani et al., 2024).

Crop sown areas compiled from statistical yearbooks at the administrative unit level (170 units comprising both counties and prefectures as shown in Fig. A1) were uniformly distributed across all cropland pixels within each unit. This assumption of homogeneous crop distribution does not reflect the actual spatial clustering of specific crops. Although several spatially explicit crop type mapping products have emerged in recent years, their utility for this study is limited by two factors. First, most existing products with relatively high resolution cover relatively short time series (typically less than 10 years), which cannot support the 21-year temporal span (2000–2020) required for this study. Second, these products predominantly focus on staple grain crops such as wheat (Dong et al., 2024), rice (Shen et al., 2023), and maize (Peng et al., 2023), while lacking coverage of the diverse crop types (e.g., vegetables, oil crops, and coarse cereals) that constitute a substantial portion of sown area in the YRB. To maintain consistency in statistical standards and minimize data inconsistencies arising from the integration of multiple heterogeneous data sources, we chose to use official sown area statistics uniformly across all crop types. As high-resolution, multi-decadal crop type mapping products with comprehensive crop coverage become available, future studies could substantially improve the spatial precision of crop-specific water demand estimation.

5.3 Implications for water resources assessment

(1) Necessity of comprehensive crop type coverage

Our results demonstrate that incomplete crop coverage not only causes substantial underestimation of absolute water demand but also misrepresents its temporal dynamics. Considering only five major crops (Scheme 1) resulted in underestimation of CWR and IWD by 33.3% and 34.2%, respectively, compared to the comprehensive 25-crop coverage (Scheme 2). More importantly, the two schemes yielded markedly different, and in some cases contradictory, representations of temporal trends. In the middle reach, the increasing rate of CWR under Scheme 2 was nearly three times that of Scheme 1 (Fig. 5c), suggesting that studies limited to major crops would substantially underestimate the intensification of agricultural water demand in this region. The two schemes even gave opposite IWD trends in the lower reach (Fig. 6c), which means that limited crop coverage could mislead water management

https://doi.org/10.5194/essd-2026-128
Preprint. Discussion started: 9 March 2026

decisions.

(2) How many crop types are sufficient?

Given the demonstrated importance of comprehensive crop coverage, a practical question arises regarding how many crop types should be considered to achieve acceptable accuracy in regional IWD assessment. To address this question, we conducted a sensitivity analysis by ranking crops according to their individual contributions to total CWR and IWD (Fig. 8). The results reveal a characteristic pattern of diminishing marginal contributions. The six crops with highest water demand (winter wheat, summer maize, spring maize, spring wheat, vegetables, and tuber crops) collectively accounted for approximately 80% of total CWR and IWD in the YRB. Extending coverage to the top 12 crops captured over 90% of the total, while 15 crops were required to reach the 95% threshold. These findings provide practical guidance for future IWD studies in similar agricultural regions. While comprehensive coverage of all crop types is ideal, studies constrained by data availability should prioritize including at least 12–15 crop types to minimize systematic underestimation. It should be noted that vegetables and tubers, crops frequently omitted in previous studies focusing exclusively on grain crops, rank among the top six contributors to basin-scale water demand, highlighting the importance of including non-grain crops in regional water assessments.

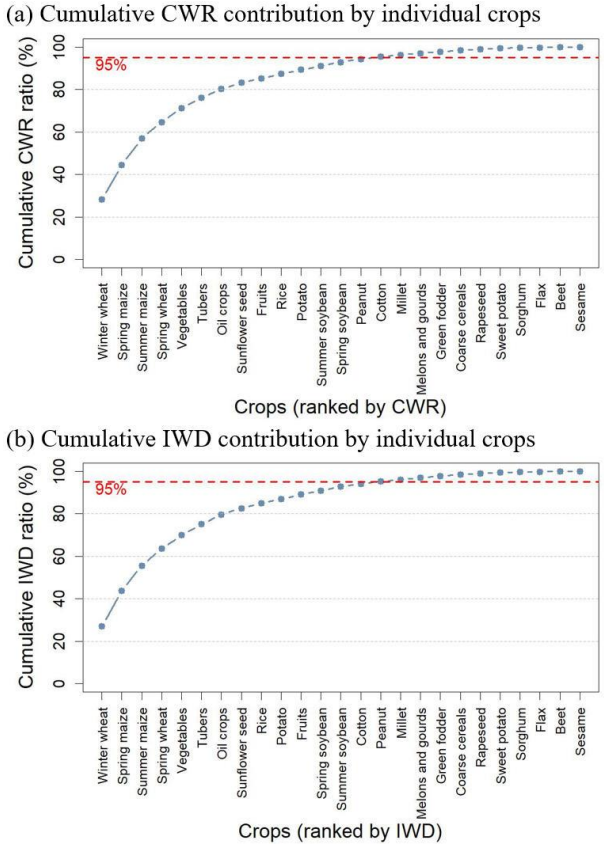

https://doi.org/10.5194/essd-2026-128
Preprint. Discussion started: 9 March 2026

Figure 8: Sensitivity analysis of cumulative CWR and IWD contributions by individual crops in the Yellow River Basin. Crops are ranked in descending order by their multi-year average (a) CWR and (b) IWD. The cumulative ratio represents the proportion of total CWR or IWD accounted for by progressively including crops from highest to lowest. The red dashed line indicates the 95% threshold.

(3) Importance of accounting for *IWUEC* dynamics

An important finding of this study is the contrasting temporal trends between CWR and IWD. While CWR exhibited a non-significant increasing trend at the basin scale with a significant increase in the upper reach (Fig. 5c), IWD showed significant decreasing trends across the basin and in both the upper and middle reaches (Fig. 6c). This divergence is primarily attributable to the substantial improvement in *IWUEC* over the study period (Fig. A3), reflecting sustained investments in irrigation infrastructure modernization and adoption of water-saving technologies across the YRB (Wang et al., 2021a). The resulting decline in IWD, despite stable or increasing crop water requirements, is consistent with observed reductions in actual agricultural water consumption reported at both basin and provincial scales (Zhu, 2025; Du et al., 2026; Lu et al., 2017). This finding suggests that assessments focusing solely on CWR without accounting for *IWUEC* dynamics would overestimate the growth in irrigation water demand. Future water resources assessments should therefore incorporate spatiotemporally explicit *IWUEC* values to accurately capture the changing relationship between crop water requirements and actual irrigation water demand.

6 Data availability

The high-resolution CWR and IWD dataset for the Yellow River Basin (2000–2020) (Tang and Zhang, 2026) is publicly available at Zenodo (https://doi.org/10.5281/zenodo.18628324) under the Creative Commons Attribution 4.0 International (CC BY 4.0) license. The dataset comprises four main directories: "CWR", "IWD", "CWR-AIA", and "IWD-AIA", where CWR and IWD represent estimates based on total crop sown area, and CWR-AIA and IWD-AIA represent estimates adjusted for actual irrigated area. Each directory contains 25 subdirectories corresponding to individual crop types (e.g., spring maize, winter wheat, cotton). Within each crop subdirectory, annual data files are stored chronologically from 2000 to 2020 in GeoTIFF format with WGS84 coordinate system and approximately 0.00417° spatial resolution. File naming follows the convention "CWR_YYYY_Crop_name.tif" (or "IWD_YYYY_Crop_name.tif") for sown area-based estimates and "CWR-AIA_YYYY_Crop_name.tif" (or "IWD-AIA_YYYY_Crop_name.tif") for irrigated area-adjusted estimates, where YYYY represents the year.

7 Conclusions

This study presents a comprehensive, high-resolution (500 m) dataset of crop water requirement (CWR) and irrigation water demand (IWD) for the Yellow River Basin covering 25 crop types over the 2000–2020 period. Two complementary versions are provided: a sown area-based version that captures the full theoretical agricultural water gap, and an irrigated area-based version that constrains estimates to actually

https://doi.org/10.5194/essd-2026-128
Preprint. Discussion started: 9 March 2026

665 irrigated cropland.

666 A central contribution of this work is the systematic quantification of how incomplete crop coverage
667 distorts both the magnitude and temporal dynamics of IWD. This practice, which remains prevalent in
668 regional water demand assessments, leads to substantial underestimation. Considering only five major
669 grain crops, as in most previous studies of the Yellow River Basin, underestimates CWR and IWD by
670 approximately 33% and 34% at the basin scale. The upper reach shows the most severe underestimation,
671 exceeding 45%. More importantly, this incomplete coverage does not merely introduce a uniform scaling
672 bias. Rather, it fundamentally misrepresents temporal trends, yielding opposite trend directions for IWD
673 in the lower reach compared to the comprehensive 25-crop estimate. This demonstrates that crop
674 coverage gaps can qualitatively distort management-relevant conclusions.

675 Our sensitivity analysis provides important and practical guidance for future studies facing data
676 constraints. At least 12 to 15 crop types are needed to capture over 90% to 95% of basin-scale water
677 demand. Notably, vegetables and tuber crops rank among the top six contributors, despite being
678 frequently omitted in grain-centric assessments. This finding highlights the necessity of incorporating
679 non-grain crops into regional water demand assessments.

680 This dataset also demonstrates the importance of accounting for the spatiotemporal dynamics of
681 irrigation water use efficiency. While CWR showed a stable to slightly increasing trend over the study
682 period, IWD showed a significant basin-wide decline. This decline was driven primarily by
683 improvements in irrigation infrastructure and water-saving technologies. Assessments that equate CWR
684 directly with IWD, which represents a common simplification, would therefore misrepresent the
685 trajectory of actual irrigation demand.

686 The evaluation framework and spatial allocation method used here are not specific to the YRB and
687 could be applied to other basins where multi-crop water demand data are needed. Users with access to
688 higher-accuracy local irrigation maps or sub-provincial efficiency data can further refine estimates by
689 applying their data to the gridded products. The dataset is publicly available at https://doi.org/
690 10.5281/zenodo.18628324.
691

https://doi.org/10.5194/essd-2026-128
Preprint. Discussion started: 9 March 2026

692 **Appendix A: Supplementary figures**

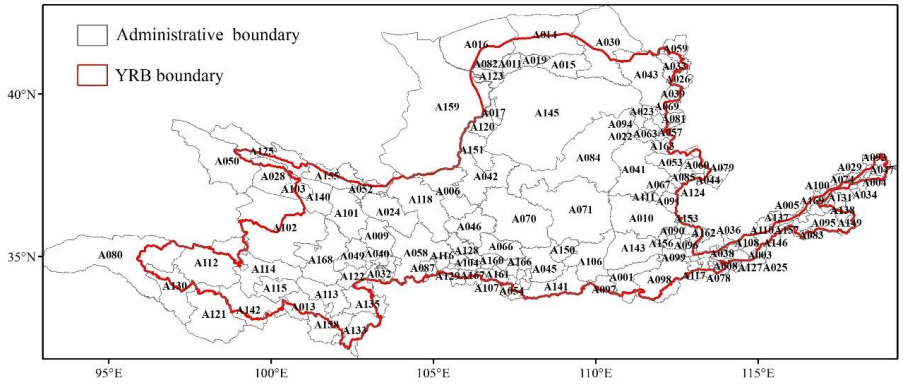

693

694 **Figure A1:** Spatial distribution of the 170 administrative units (counties or prefectures) used for crop-
695 specific sown area compilation in the Yellow River Basin.

696

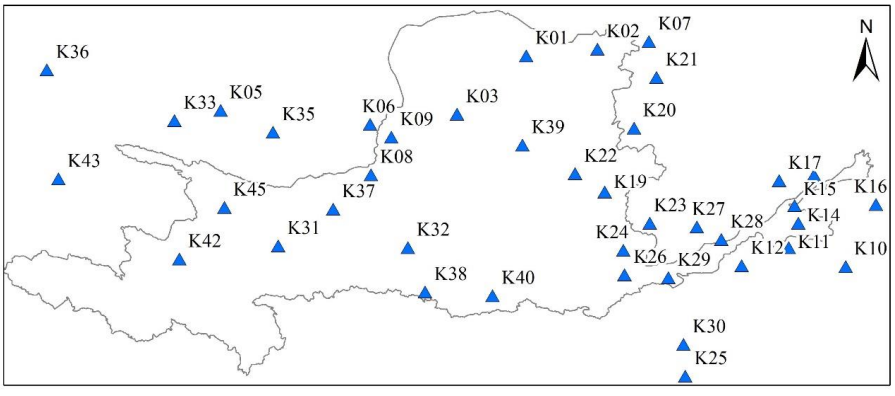

697

698 **Figure A2:** The distribution of 45 observation stations for crop coefficients.

699

https://doi.org/10.5194/essd-2026-128
Preprint. Discussion started: 9 March 2026

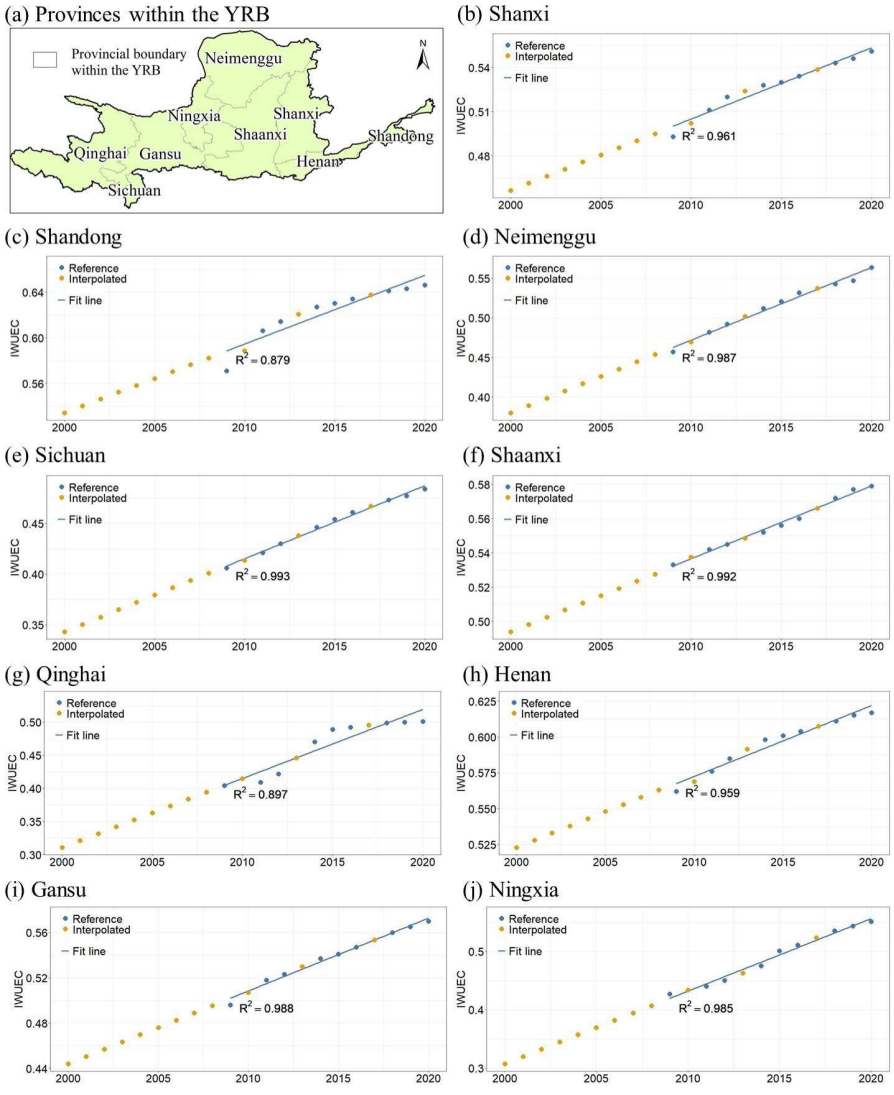

Figure A3: Provincial irrigation water use efficiency coefficients (*IWUEC*) from 2000 to 2020. Blue points indicate reference data from official statistics; orange points represent interpolated values based on linear regression fitted to the reference period (2009–2020).

https://doi.org/10.5194/essd-2026-128
Preprint. Discussion started: 9 March 2026

Author contributions

ST implemented the methodology, processed the data, developed the code, performed the analysis, and contributed to manuscript writing. HZ conceived and designed the study, wrote the original draft, obtained funding support, and contributed to the code development. ZL, LZ, and JW contributed to data collection and preparation. XS, LL, YD, and QL provided scientific advice and reviewed the manuscript.

Competing interests

The authors declare that they have no conflict of interest.

Acknowledgements

This work was funded by Xinjiang Key Laboratory of Water Cycle and Utilization in Arid Zone, Xinjiang Institute of Ecology and Geography, Chinese Academy of Sciences (Grant No. XJYS0907-2024-zd-04), National Natural Science Foundation of China (Grants 42471146 and U2243217), and the Open Project of Middle Yarlung Zangbo River Natural Resources Observation and Research Station (Grant No. YJZ-2025-003).

References

Alimagham, S., van Loon, M. P., Ramirez-Villegas, J., Adjei-Nsiah, S., Baijukya, F., Bala, A., Chikowo, R., Silva, J. V., Soulé, A. M., and Taulya, G.: Climate change impact and adaptation of rainfed cereal crops in sub-Saharan Africa, European Journal of Agronomy, 155, 127137, 2024.

Allen, R. G., Pereira, L. S., Raes, D., and Smith, M.: Crop evapotranspiration-Guidelines for computing crop water requirements-FAO Irrigation and drainage paper 56, Fao, Rome, 300, D05109, 1998.

Archer, D. R., Forsythe, N., Fowler, H. J., and Shah, S. M.: Sustainability of water resources management in the Indus Basin under changing climatic and socio economic conditions, Hydrol Earth Syst Sc, 14, 1669-1680, 2010.

National Earth System Science Data Center: https://www.geodata.cn/dlsagri/, last access: October 25, 2023.

Chai, Q., Gan, Y., Zhao, C., Xu, H.-L., Waskom, R. M., Niu, Y., and Siddique, K. H.: Regulated deficit irrigation for crop production under drought stress. A review, Agronomy for sustainable development, 36, 3, 2016.

Chen, X., Huang, Q., Xiong, Y., Yang, Q., Li, H., Hou, Z., and Huang, G.: Tracking the spatio-temporal change of the main food crop planting structure in the Yellow River Basin over 2001–2020, Computers and Electronics in Agriculture, 212, 108102, 2023.

De Wrachien, D., Schultz, B., and Goli, M. B.: Impacts of population growth and climate change on food production and irrigation and drainage needs: A world-wide view, Irrigation and Drainage, 70, 981-995, https://doi.org/10.1002/ird.2597, 2021.

Döll, P. and Siebert, S.: Global modeling of irrigation water requirements, Water resources

https://doi.org/10.5194/essd-2026-128
Preprint. Discussion started: 9 March 2026

research, 38, 8-1-8-10, 2002.
Dong, J., Pang, Z., Fu, Y., Peng, Q., Li, X., and Yuan, W.: Annual winter wheat mapping dataset in China from 2001 to 2020, Scientific Data, 11, 1218, 2024.
Du, B., Yang, Z., Guo, H., Zhang, H., Ma, X., Zhou, Q., Li, J., Zhou, Z., Tang, Y., and Yang, Y.: Analysis of changes and influencing factors of effective utilization coefficient of farmland irrigation water in Ningxia, Water Saving Irrigation, 2026.
Duan, A., Sun, J., Liu, Y., Xiao, J., Liu, Q., and Qi, X.: Irrigation Water Quota for Main Crops in Northern China, China Agricultural Science and Technology Press, Beijing2004.
ESA: Land Cover CCI Product User Guide Version 2, 2017.
Fan, S., Liu, T., Zou, M., Fang, Y., Niu, J., and Kang, S.: Spatiotemporal dynamics and driving factors of irrigation water demands in China, Agricultural Water Management, 312, 109450, https://doi.org/10.1016/j.agwat.2025.109450, 2025.
Fang, L. and Li, J.: Ecological Protection and High Quality Development of the Yellow River Basin from the Perspective of Food Security, Chinese Journal of Environmental Management, 2019.
AQUASTAT - Irrigated crop calendars: https://www.fao.org/aquastat/en/databases/crop-calendar/, last access: May 13, 2024.
Frenken, K. and Gillet, V.: Irrigation water requirement and water withdrawal by country, FAO, Rome, Italy, 2012.
Friedl, M. and Sulla-Menashe, D.: MODIS/Terra+Aqua Land Cover Type Yearly L3 Global 500m SIN Grid V061 [dataset], 2022.
Fu, J., Wang, W., Zaitchik, B., Nie, W., Fei, E. X., Miller, S. M., and Harman, C. J.: Critical role of irrigation efficiency for cropland expansion in western China arid agroecosystems, Earth's Future, 10, e2022EF002955, 2022.
Holm, S.: A simple sequentially rejective multiple test procedure, Scandinavian journal of statistics, 65-70, 1979.
Hou, Y., Wang, S., Song, S., Chen, P., and Wu, X.: Crop irrigation water requirements mismatch the actual water allocation in the anthropogenic-regulated Yellow River Basin, Journal of Hydrology: Regional Studies, 61, 102715, 2025.
Hu, S., Chen, Q., Zhang, G., and Li, M.: Trend analysis of water resources utilization in the Yellow River Basin, Journal of Water Resources & Water Engineering, 2012.
Hung, F., Chiarelli, D. D., Famiglietti, J. S., and Müller, M. F.: Downscaled global 60-meter resolution estimates of irrigation water sources (2000–2015), Scientific Data, 12, 1632, 2025.
Jägermeyr, J., Gerten, D., Heinke, J., Schaphoff, S., Kummu, M., and Lucht, W.: Water savings potentials of irrigation systems: global simulation of processes and linkages, Hydrol Earth Syst Sc, 19, 3073-3091, 2015.
Jia, K., Zhang, W., Xie, B., Xue, X., Zhang, F., and Han, D.: Does climate change increase crop water requirements of winter wheat and summer maize in the lower reaches of the Yellow River Basin?, International Journal of Environmental Research and Public Health, 19, 16640, 2022.
Kadiresan, K. and Khanal, P. R.: Rethinking irrigation for global food security, Irrigation and drainage, 67, 8-11, 2018.
Liu, F., Chen, S., Dong, P., and Peng, J.: Spatial and temporal variability of water discharge in

https://doi.org/10.5194/essd-2026-128
Preprint. Discussion started: 9 March 2026

788 the Yellow River Basin over the past 60 years, J. Geogr. Sci., 22, 1013-1033, 2012.
789 Liu, H., Gong, P., Wang, J., Clinton, N., Bai, Y., and Liang, S.: Annual dynamics of global land
790 cover and its long-term changes from 1982 to 2015, Earth System Science Data, 12, 1217-
791 1243, 2020.
792 Liu, Q. and Yang, Z.: Quantitative estimation of the impact of climate change on actual
793 evapotranspiration in the Yellow River Basin, China, Journal of Hydrology, 395, 226-234,
794 2010.
795 Liu, X., Shen, Y., Guo, Y., Li, S., and Guo, B.: Modeling demand/supply of water resources in
796 the arid region of northwestern China during the late 1980s to 2010, J. Geogr. Sci., 25, 573-
797 591, 2015.
798 Liu, Y., Wang, L., Ni, G., and Cong, Z.: Spatial distribution characteristics of irrigation water
799 requirement for main crops in China, Transactions of the Chinese Society of Agricultural
800 Engineering, 25, 6-12, 2009.
801 Liu, Y., Lin, Y., Huo, Z., Zhang, C., Wang, C., Xue, J., and Huang, G.: Spatio-temporal variation
802 of irrigation water requirements for wheat and maize in the Yellow River Basin, China,
803 1974–2017, Agricultural Water Management, 262, 107451, 2022.
804 Liu, Z., Wu, H., Wu, Y., Wang, Y., Li, Q., and Zhang, H.: Investigating the ability of state-of-
805 the-art remote sensing datasets in capturing the spatiotemporal patterns of cropland area:
806 implications for agricultural monitoring in the largest river basin of China's arid region,
807 Smart Agricultural Technology, 101580, 2025.
808 Lu, L., Li, X., and Huang, X.: Study on agricultural water-saving irrigation efficiency in Henan,
809 Water Resources & South to North Water Diversion, 20-21, 2017.
810 Lutz, A., Immerzeel, W., Siderius, C., Wijngaard, R., Nepal, S., Shrestha, A., Wester, P., and
811 Biemans, H.: South Asian agriculture increasingly dependent on meltwater and
812 groundwater, Nature Climate Change, 1-8, 2022.
813 Mingzhong, C.: Great Achievements on the Project of "Research and Demonstration of Water-
814 Saving Agriculture Technology" and Prospect to"The Tenth-Five Year" National
815 Programming, Review of China Agricultural Science and Technology, 2000.
816 Mkuhlani, S., Bendito, E. G., Tofa, A. I., Aliyu, K. T., Shehu, B. M., Kreye, C., and Chemura,
817 A.: Spatial and temporal distribution of optimal maize sowing dates in Nigeria, Plos one,
818 19, e0300427, 2024.
819 China Water-Saving Irrigation Network: www.jsgg.com.cn, last access: June 4, 2025.
820 Niu, C., Qi, Y., Guo, A., and Chang, J.: Grain yield and food security evaluation in the yellow
821 river basin under climate change and water resources constraints, Frontiers in Water, 4,
822 908945, 2022.
823 Peng, Q., Shen, R., Li, X., Ye, T., Dong, J., Fu, Y., and Yuan, W.: A twenty-year dataset of high-
824 resolution maize distribution in China, Scientific Data, 10, 658, 2023.
825 Peng, S., Wang, Y., and Jiang, J.: Study on the relationship between irrigation water requirement
826 and drought in the main irrigation area of the Yellow River basin, Yellow River, 39, 5-10,
827 2017.
828 Peng, S., Zheng, X., Yan, D., and Shang, W.: New situation and countermeasures of water
829 resources supply and demand in the Yellow River Basin, China Water Resour, 18, 18-20,
830 2021.
831 Pirmoradian, N., Saadati, Z., Rezaei, M., and Khaledian, M. R.: Simulating water productivity

https://doi.org/10.5194/essd-2026-128
Preprint. Discussion started: 9 March 2026

of paddy rice under irrigation regimes using AquaCrop model in humid and semiarid regions of Iran, Applied Water Science, 10, 1-8, 2020.

Potapov, P., Turubanova, S., Hansen, M. C., Tyukavina, A., Zalles, V., Khan, A., Song, X.-P., Pickens, A., Shen, Q., and Cortez, J.: Global maps of cropland extent and change show accelerated cropland expansion in the twenty-first century, Nature Food, 3, 19-28, 2022.

Qin, Y., Abatzoglou, J. T., Siebert, S., Huning, L. S., AghaKouchak, A., Mankin, J. S., Hong, C., Tong, D., Davis, S. J., and Mueller, N. D.: Agricultural risks from changing snowmelt, Nature Climate Change, 10, 459-465, 2020.

Shen, R., Pan, B., Peng, Q., Dong, J., Chen, X., Zhang, X., Ye, T., Huang, J., and Yuan, W.: High-resolution distribution maps of single-season rice in China from 2017 to 2022, Earth System Science Data Discussions, 2023, 1-27, 2023.

Shen, Y., Li, S., Chen, Y., Qi, Y., and Zhang, S.: Estimation of regional irrigation water requirement and water supply risk in the arid region of Northwestern China 1989–2010, Agricultural water management, 128, 55-64, 2013.

Siebert, S. and Döll, P.: The Global Crop Water Model (GCWM): Documentation and first results for irrigated crops, Univ., Inst. of Physical Geography, 2008.

Siebert, S., Burke, J., Faures, J.-M., Frenken, K., Hoogeveen, J., Döll, P., and Portmann, F. T.: Groundwater use for irrigation–a global inventory, Hydrol Earth Syst Sc, 14, 1863-1880, 2010.

Tang, S. and Zhang, H.: A 500-m crop water requirement and irrigation water demand dataset for 25 crop types in the Yellow River Basin (2000–2020), Zenodo [dataset], 10.5281/zenodo.18628324, 2026.

Tu, Y., Wu, S., Chen, B., Weng, Q., Bai, Y., Yang, J., Yu, L., and Xu, B.: A 30 m annual cropland dataset of China from 1986 to 2021, Earth System Science Data, 16, 2297-2316, 2024.

Uniyal, B. and Dietrich, J.: Modifying automatic irrigation in swat for plant water stress scheduling, Agricultural Water Management, 223, 105714, 2019.

Wada, Y., Wisser, D., Eisner, S., Flörke, M., Gerten, D., Haddeland, I., Hanasaki, N., Masaki, Y., Portmann, F. T., and Stacke, T.: Multimodel projections and uncertainties of irrigation water demand under climate change, Geophys. Res. Lett., 40, 4626-4632, 2013.

Wang, J., Li, G., and Song, C.: Development countermeasures and suggestions for highly-efficient water-saving irrigation of the Yellow River irrigation area, Journal of Irrigation and Drainage, 40, 111-114, 2021a.

Wang, W., Shao, Q., Peng, S., Xing, W., Yang, T., Luo, Y., Yong, B., and Xu, J.: Reference evapotranspiration change and the causes across the Yellow River Basin during 1957–2008 and their spatial and seasonal differences, Water resources research, 48, 2012.

Wang, X., Chen, D., Pang, G., Gou, X., and Yang, M.: Historical and future climates over the upper and middle reaches of the Yellow River Basin simulated by a regional climate model in CORDEX, Clim. Dyn., 56, 2749-2771, 2021b.

Wang, Y., Wang, W., Peng, S., Jiang, G., and Wu, J.: The relationship between irrigation water demand and drought in the Yellow River basin, Proceedings of the International Association of Hydrological Sciences, 374, 129-136, 2016.

Wu, J., Gao, X., Giorgi, F., and Chen, D.: Changes of effective temperature and cold/hot days in late decades over China based on a high resolution gridded observation dataset, International Journal of Climatology, 37, 788-800, 2017.

https://doi.org/10.5194/essd-2026-128
Preprint. Discussion started: 9 March 2026

876 Xu, H., Tian, Z., He, X., Wang, J., Sun, L., Fischer, G., Fan, D., Zhong, H., Wu, W., and Pope,
877 E.: Future increases in irrigation water requirement challenge the water-food nexus in the
878 northeast farming region of China, Agricultural Water Management, 213, 594-604, 2019.
879 Xu, Y., Yu, L., Peng, D., Zhao, J., Cheng, Y., Liu, X., Li, W., Meng, R., Xu, X., and Gong, P.:
880 Annual 30-m land use/land cover maps of China for 1980–2015 from the integration of
881 AVHRR, MODIS and Landsat data using the BFAST algorithm, Science China Earth
882 Sciences, 63, 1390-1407, 2020.
883 Xuan, F., Dong, Y., Li, J., Li, X., Su, W., Huang, X., Huang, J., Xie, Z., Li, Z., Liu, H., Tao, W.,
884 Wen, Y., and Zhang, Y.: Mapping crop type in Northeast China during 2013–2021 using
885 automatic sampling and tile-based image classification, Int. J. Appl. Earth Obs. Geoinf.,
886 117, 103178, https://doi.org/10.1016/j.jag.2022.103178, 2023.
887 Yan, H., Liu, F., Qin, Y., Niu, Z. e., Doughty, R., and Xiao, X.: Tracking the spatio-temporal
888 change of cropping intensity in China during 2000–2015, Environ. Res. Lett., 14, 035008,
889 2019.
890 Yang, J. and Huang, X.: The 30m annual land cover dataset and its dynamics in China from
891 1990 to 2019, Earth Syst. Sci. Data, 13, 3907-3925, 10.5194/essd-13-3907-2021, 2021.
892 Yang, T., Xu, C.-Y., Shao, Q., Chen, X., Lu, G.-H., and Hao, Z.-C.: Temporal and spatial
893 patterns of low-flow changes in the Yellow River in the last half century, Stochastic
894 Environmental Research and Risk Assessment, 24, 297-309, 2010.
895 Zha, H., Zhang, F., Zhang, H., Tang, S., Zhang, L., and Luo, L.: Unraveling the Distinct Roles
896 of Snowmelt and Glacier-Melt on Agricultural Water Availability: A Novel Indicator and
897 Its Application in a Glacierized Basin of China's Arid Region, Water Resources Research,
898 61, e2023WR036898, 2025.
899 Zhang, L., Xie, Y., Zhu, X., Ma, Q., and Brocca, L.: CIrrMap250: annual maps of China's
900 irrigated cropland from 2000 to 2020 developed through multisource data integration, Earth
901 System Science Data, 16, 5207-5226, 2024.
902 Zhao, J., Wu, L., Wang, X., Yu, Y., and Huang, K.: High-resolution water footprints of major
903 crops in China from cities to grids, Scientific Reports, 2025.
904 Zhu, J.: Decomposition of Drivers, Multi-Scenario Prediction, and Water Saving Pathways for
905 Agricultural Water Use Evolution in the Yellow River Basin, Master's thesis, Jiangsu
906 University of Science and Technology, 2025.
907 Zhuo, L., Mekonnen, M. M., Hoekstra, A. Y., and Wada, Y.: Inter-and intra-annual variation of
908 water footprint of crops and blue water scarcity in the Yellow River basin (1961–2009),
909 Advances in water resources, 87, 29-41, 2016.

910